Duplex structure of double-stranded RNA provides stability against hydrolysis relative to single-stranded RNA

Ke Zhang, Joseph Hodge, Anamika Chatterjee, Tae Seok Moon, Kimberly M. Parker*

Department of Energy, Environmental & Chemical Engineering,

Washington University in St. Louis, St. Louis, Missouri 63130, United States

* Corresponding author: kmparker@wustl.edu, phone: (314) 935-3461.

Words: 5,198

Figures: 4 (1800 word-equivalents)

Total word-equivalents: 6,998

Key words: double-stranded RNA, alkaline hydrolysis, single-stranded RNA, secondary structure, base-catalyzed hydrolysis

Abstract

Phosphodiester bonds in the backbones of double-stranded (ds)RNA and single-stranded (ss)RNA are known to undergo alkaline hydrolysis. Consequently, dsRNA agents used in emerging RNA interference (RNAi) products have been assumed to exhibit low chemical persistence in solutions. However, the impact of the duplex structure of dsRNA on alkaline hydrolysis has not yet been evaluated. In this study, we demonstrated dsRNA undergoes orders-of-magnitude slower alkaline hydrolysis than ssRNA. Furthermore, we observed dsRNA remains intact for multiple months at neutral pH, challenging the assumption that dsRNA is chemically unstable. In systems enabling both enzymatic degradation and alkaline hydrolysis of dsRNA, we found increasing pH effectively attenuated enzymatic degradation without inducing alkaline hydrolysis that was observed for ssRNA. Overall, our findings demonstrated, for the first time, that key degradation pathways of dsRNA significantly differ from those of ssRNA. Consideration of the unique properties of dsRNA will enable greater control of dsRNA stability in emerging RNAi technology and more accurate assessment of its fate in environmental and biological systems, as well as provide insights in broader application areas including dsRNA isolation, detection and inactivation of dsRNA viruses, and prebiotic molecular evolution.

Synopsis:

Slow hydrolysis of dsRNA molecules, including those used in RNAi products, may contribute to their chemical persistence in environmental and biological systems.

Introduction

RNA interference (RNAi) is a biological process in which double-stranded RNA (dsRNA) directs the degradation of homologous messenger RNA (mRNA), preventing the synthesis of a specific target protein.[1] In recent years, RNAi has been utilized in numerous applications across several fields. In medicine, dsRNA and shorter duplex RNA known as small interfering RNA (siRNAs) have been developed as therapeutic agents with antitumor and antiviral properties.[2,3] In agriculture, several RNAi-based products have been developed using dsRNA as active agents (i.e., dsRNA pesticides) to protect crops from pests, including insects and fungi.[4] These agricultural RNAi-based products include both dsRNA generated by dsRNA-expressing genetically modified crops[5] and dsRNA produced in vitro or by dsRNA-expressing bacteria prior to application via spray or irrigation water.[6-9]

The application of RNAi-based products raises the importance of developing a fundamental understanding of the chemical stability of dsRNA molecules. Like single-stranded RNA (ssRNA), chemical degradation of dsRNA may in principle occur by hydrolysis of the phosphodiester bonds that comprise the backbone of both molecules, in particular under alkaline conditions.[10] However, the double-helix structure of dsRNA has been proposed to impede phosphodiester bond hydrolysis,[11] in agreement with evidence that self-complementary regions in ssRNA resist hydrolysis catalyzed by certain chemicals (e.g., lead, polyvinylpyrrolidone).[12-16] These studies are limited in their application to dsRNA products because the duplex self-complementary regions in ssRNA are usually short (< 20 base pairs, bp) and often contain mismatched base pairs. Consequently, the effect of the duplex structure of dsRNA generated from long (e.g., > 100 bp)[17] complementary ssRNA strands on alkaline hydrolysis rates has yet to be experimentally validated.

As dsRNA stability has yet to be directly characterized, the possibility for the structure of dsRNA to alter its reactions relative to ssRNA is frequently neglected in discussions of the application and risk assessment of RNAi products. For example, dsRNA pesticides are thought to be less effective in insect species with high gut pH[18,19] due to presumed alkaline hydrolysis.[20-26] In addition, following established protocols to store ssRNA products to avoid alkaline hydrolysis,[27-31] dsRNA products typically are also stored in solutions at circumneutral pH.[32,33] The assumption that chemical hydrolysis

63 contributes to rapid dsRNA degradation in biological and environmental solutions is also pervasive in
64 the assessments of the potential risks posed by dsRNA products to humans and other non-target
65 organisms. The United States Environmental Protection Agency (EPA) Scientific Advisory Panel on
66 RNAi technology based their analysis of the stability of dsRNA in the guts of non-target organisms on
67 the assumptions that "RNA is an intrinsically unstable molecule even in normal aqueous conditions no
68 matter what structural conformation (single-stranded or double-stranded) it assumes"[34] and that "both
69 acidic and basic conditions can drive intra-strand hydrolysis of RNA chains irrespective of the structural
70 conformation of that molecule."[34] The chemical degradation of dsRNA pesticides in receiving
71 environments (e.g., soil and surface water) has also been assumed to reduce their potential to result in
72 adverse ecological impact,[34,35] including one study that indicated chemical degradation of dsRNA
73 pesticides might exceed biological degradation in surface water.[35]

74 In this study, we provide the first characterization of the chemical stability of dsRNA at neutral
75 and alkaline pH directly applicable to the fate of dsRNA products at environmental and biological
76 systems. We first evaluated the impact of the duplex structure of dsRNA on its alkaline hydrolysis
77 relative to ssRNA and corroborated our results using several complementary techniques. Next, we
78 tested the degradation of both ssRNA and dsRNA molecules at circumneutral pH. Finally, we evaluated
79 the overall degradation rates of ssRNA and dsRNA due to both alkaline and enzymatic hydrolysis as a
80 function of pH to determine the pH of optimum stability for both molecules. We discussed the
81 implications of our findings for RNAi technology development and risk assessment, as well as wide-
82 ranging contexts, including RNA isolation protocols, dsRNA virus quantification and inactivation, and
83 prebiotic molecular evolution.

84

85 **Materials and Methods**

86 *Materials*

87 Chemicals, kits, and supplies used in this study are described in Section S1. We synthesized
88 dsRNA (100 and 1000 bp) and ssRNA (106 and 1006 nucleotides, nt) using the in vitro T7 polymerase
89 reaction. The ssRNA molecules have the same sequence as the sense strand of dsRNA molecules, with

the exception of one experiment using the antisense ssRNA (**Fig. S8**), but have an additional 6 nt sequence (GGGAGA) in the 5'-end. The synthesis method and sequence of these RNA molecules are indicated in Section S2.

RNase-free Protocol

We conducted our experiments while minimizing the presence of RNase (details provided in Section S3). At all stages, we used RNase-free disposable supplies (e.g., tubes and pipettor tips), glassware baked at 450 ºC for 4 h, or reusable plasticware treated with 0.1% diethylpyrocarbonate (DEPC). Buffers were prepared with ultrapure water, autoclaved, and aliquoted before storage at 4 °C (for less than a week) or at -80°C. RNA was synthesized and handled in a laminar hood prior to analysis.

RNA Incubation

RNA was incubated in 20 μL solutions (exception: 100 μL for HPLC analysis) containing 20 mM NaCl and 3 mM of buffer salt selected based on the experimental pH (MOPS for pH 7.0-8.0, borate for pH 9.0, bicarbonate for pH 10.0-11.0, and phosphate for pH 12.0-12.4). We used 1.5 mL Protein LoBind tubes for experiments because dsRNA negligibly adsorbs to the tube walls.[36]

When indicated, formamide was used to denature dsRNA immediately prior to agarose gel electrophoresis.[37] We mixed the dsRNA solution with pure formamide at a volume ratio of 2:3 in a chemical fume hood and heated the mixture at 65 °C for 2 min, followed by chilling at 5 °C for 5 min. The addition of formamide increased the sample volume from 20 μL to ~50 μL, of which 20 μL was then loaded on agarose gels for analysis.

For experiments using human saliva RNase, we collected the saliva (~1 mL) in 1.5 mL Protein LoBind tubes at 0.5 h after brushing teeth. To separate RNase from mucus,[38,39] we centrifuged the saliva at 21,100 g for 5 min and collected the supernatant (the top ¾ by volume) for a total of 3 cycles. The resultant liquid was stored at -20 °C until use. For experiments using soil solution RNase, we mixed a slurry prepared with 50 g fine sandy loam soil (characterized previously[40]) and 50 mL sterile water in an uncovered 250 mL Erlenmeyer flask using a stir bar (1000 rpm) at 24 °C for 2 days. We then centrifuged the slurry at 21,100 g for 1 min and collected the supernatant. The supernatant was stored at 4 °C for < 24 h before used as soil solution RNase.

Analysis of ssRNA and dsRNA

Concentrations of intact ssRNA and dsRNA were determined by measuring ultraviolet (UV) light absorbance using a NanoDrop 2000c spectrophotometer (Thermo Fisher Scientific), which can quantify nucleic acid concentrations above 2 ng/μL according to the manufacturer. To convert UV absorbance at 260 nm to concentration, we applied extinction coefficients of 0.0214 and 0.0266 $(ng/\mu L)^{-1} \cdot cm^{-1}$ for dsRNA and ssRNA, respectively.[41] The difference in their extinction coefficients also allowed us to determine conditions that resulted in dsRNA denaturation by detecting an increase in UV absorbance (**Fig. S9**).

The loss of intact ssRNA and dsRNA was analyzed by agarose gel electrophoresis (followed by gel image analysis, Section S4) to measure changes in RNA length without pretreatment (e.g., removal of organic matter). Quantitative reverse transcription polymerase chain reaction (RT-qPCR) was used as a supplementary analytical method for intact ssRNA and dsRNA (Sections S5). In both cases, the RNA type for standards corresponded to the type of the samples. Product analysis was conducted using high-performance liquid chromatography (HPLC) with UV detection (Section S6).

Statistical Tests

Each data point represents an independently prepared sample, with the number of samples prepared per time point indicated in the figure captions. Differences in hydrolysis rates and RNA concentrations were evaluated for statistical significance using GraphPad Prism 7.04 and Excel (Version 1911, unpaired Student's *t*-test), respectively, with a confidence level was set as $p \leq 0.05$.

Results and Discussion

1. Alkaline hydrolysis of ssRNA and dsRNA

The primary structure of RNA consists of ribonucleotide monomers connected by phosphodiester bonds. Phosphodiester bonds undergo alkaline hydrolysis (also known as base-catalyzed hydrolysis or hydroxide-mediated hydrolysis) upon deprotonation of 2'-hydroxyl group (pK_a = ~13) to generate a nucleophilic 2'-oxyanion (**Fig. 1A**).[42,43] The 2'-oxyanion attacks the electrophilic phosphorus atom, leading to the cleavage of the phosphodiester linkage.[43] Degradation of ssRNA is

well-established to occur via alkaline hydrolysis;[10,44] however, the possibility for dsRNA to degrade via a similar pathway has not been experimentally studied to date. We hypothesized that the rigidity of the dsRNA duplex may hinder the requisite intramolecular attack from initiating cleavage of the phosphodiester linkage.

To evaluate how the duplex structure of dsRNA affects its alkaline hydrolysis, we first compared the degradation rates of 100 bp dsRNA and 106 nt ssRNA at pH 12.0 (**Fig. 1B**). We confirmed that dsRNA didn't denature at this pH using UV absorbance (**Fig. S9**). The ssRNA molecules used throughout this study are identical to the sense strand of the dsRNA molecule, with the exception of additional 6 nt due to the synthesis method (Section S2). To assess the loss of the intact molecule, we used gel electrophoresis, which distinguishes products of ssRNA or dsRNA degradation that are shorter than ~70%-80% of their initial length from the intact molecules (Section S4). Using this method, we observed that the 106 nt ssRNA degraded following apparent first-order kinetics with an observed rate constant (k_{obs}) of $2.5(\pm0.2)\times10^{-3}$ min^{-1} over a period of 4 hours (**Fig. 1C**). In contrast, the 100 bp dsRNA did not undergo observable degradation over the same time period, resulting in an observed rate constant ($k_{obs} = 1.8(\pm1.0)\times10^{-4}$ min^{-1}) that was not significantly different from zero ($p = 0.09$). Comparing the rate constant for dsRNA hydrolysis to that for ssRNA hydrolysis indicates that dsRNA was more resistant to alkaline hydrolysis than ssRNA ($p < 0.0001$).

The dsRNA active agents used in RNAi technologies can be up to an order of magnitude larger than the 100 bp molecule tested above (**Table S2**). To evaluate whether longer dsRNA molecules would also show enhanced stability against alkaline hydrolysis relative to ssRNA, we completed similar experiments as detailed above using 1000 bp dsRNA and 1006 nt ssRNA (**Fig. 1D**). We observed that 1006 nt ssRNA degraded following apparent first-order kinetics ($k_{obs} = 2.39(\pm0.06)\times10^{-2}$ min^{-1}) **(Fig. 1E**) and was below the lowest quantifiable concentration of this method (3.1 ng/μL) after 80 min. The 1006 nt ssRNA degraded approximately an order of magnitude faster than the 106 nt ssRNA, likely corresponding to the 10-fold greater number of phosphodiester bonds. We also determined that the complementary ssRNA strand also hydrolyzes with a comparable rate constant ($k_{obs} = 1.75(\pm0.18)\times10^{-2}$ min^{-1}) (**Fig. S8**). In contrast, the 1000 bp dsRNA remained significantly more stable than ssRNA ($p <$

0.0001), indicating that the increased stability of dsRNA against alkaline hydrolysis may be consistent across common sizes of dsRNA products (**Fig. 1**). This result was replicated using dsRNA generated by annealing the individual complementary ssRNA strands (**Fig. S8**), indicating that the resistance of dsRNA to alkaline hydrolysis was independent of the synthesis method.

These results provided the first evidence that dsRNA is more resistant to alkaline hydrolysis than ssRNA. Notably, due to pH- and temperature-dependent folding,[45,46] ssRNA often contains some double-stranded regions, which have been most commonly studied under physiological conditions (i.e., 37 °C, neutral pH). The ssRNA molecules used herein might also fold (**Fig. S2**).[47] However, despite this potential for ssRNA molecules to include some double-stranded regions, we still observed very different hydrolysis rates for ssRNA and dsRNA, potentially due to hydrolysis occurring in single-stranded loop regions within the ssRNA molecule that are not present in dsRNA.

We next conducted additional experiments to further confirm that individual strands within the dsRNA molecules remained intact throughout the duration of our experiment. Because the dsRNA molecules were not denatured during analysis, the dsRNA strands could conceivably hydrolyze but remain held together by hydrogen bonds between the two strands, resulting in migration into the gel to the same distance as the initial molecule. To test if the strands of dsRNA were both intact, we denatured the dsRNA using formamide (confirmed in **Fig. S10**)[37] after the alkaline incubation but before gel analysis. The measured concentrations of denatured strands of the 1000 bp dsRNA molecule remained approximately constant for the duration of the experiment (**Fig. 1D**), indicating degradation of the individual strands was not detected by gel electrophoresis.

To confirm that dsRNA degraded more slowly than ssRNA, we applied a complementary approach, RT-qPCR. Whereas common applications of qPCR analysis (e.g., relative quantification of gene expression level analysis)[48,49] typically require short amplification regions (e.g., 75-150 bp)[50] so that the PCR amplification efficiency can be assumed to be 100% (e.g., to apply the $2^{-\Delta\Delta Ct}$ method)[51], we applied RT-qPCR for absolute quantification with a standard curve analyzed with each measurement, which has no requirement on amplification efficiency. Hence, we were able to amplify the entire sequence (i.e., the sense strand of the 1000 bp dsRNA as well as the entire 1006 nt ssRNA excepting

198 the 6 nt cap). Consequently, whereas the gel electrophoresis method requires the degradation products
199 to be 20-30% shorter than the intact molecule, the RT-qPCR method is expected to detect degradation
200 even if only a few nucleotides are lost. In addition to being more sensitive than gel electrophoresis, RT-
201 qPCR also provides additional confirmation beyond our formamide experiments that the two strands in
202 the dsRNA molecule remain intact. At pH 12.0, the degradation kinetics of both ssRNA and dsRNA
203 molecules were substantially more rapid when quantified using RT-qPCR than the gel electrophoresis
204 (**Fig. 1**). After 1006 nt ssRNA was degraded for 60 min, only 9.5(±1.0)% remained when measured by
205 RT-qPCR (**Fig. 1F**), whereas 23.5(±2.3)% remained after the same time period when measured by the
206 gel electrophoresis approach (**Fig. 1D**). In addition, whereas the degradation of dsRNA was not detected
207 by gel electrophoresis, the intact molecules were reduced to 74.5(±7.4)% of their initial values after 60
208 min when analyzed by RT-qPCR. This finding may indicate the ends of the dsRNA molecule are more
209 susceptible to degradation than the interior of the molecule, as degradation of the ends would be
210 detectable by RT-qPCR but not gel electrophoresis.

211 Whereas the above methods all demonstrated that dsRNA degrades more slowly than ssRNA,
212 they only monitor loss of the intact molecule and do not provide direct evidence that alkaline hydrolysis
213 is the specific pathway responsible for this difference. To investigate the specific mechanism that differs
214 between the two molecules, we analyzed the generation of the final end products, nucleotide monomers
215 (nucleoside monophosphate), using HPLC (**Fig. 1G**). Alkaline hydrolysis of RNA leads to the
216 production of 2',3'-cyclic monophosphate nucleotide[52] that further hydrolyzes to 2' and 3'-
217 mononucleotides at a ratio of 0.85 (2':3').[53] In contrast, enzymatic hydrolysis generates the 3'-
218 mononucleotide as the sole product.[52,54,55] We identified 2' and 3'-adenosine monophosphate (AMP) in
219 the hydrolysates of 1006 nt ssRNA and 1000 bp dsRNA at pH 12.0 (**Fig. 1G**). At the end of the
220 hydrolysis reaction (92 h), the ratios of 2'-AMP to 3'-AMP in hydrolysates were 0.86(±0.03) and
221 0.80(±0.05) for ssRNA and dsRNA, respectively, supporting alkaline hydrolysis as the dominant
222 degradation reaction for both molecules. Even after 92 h of incubation at pH 12.0, only a small fraction
223 of the AMP in the RNA molecules (i.e., 3.7% total AMP in ssRNA) was recovered as nucleoside
224 monophosphate. The low yield of hydrolysis products relative to the loss of the intact molecule

(e.g., >87.5 % loss of intact 1006 nt ssRNA at 2 h, **Fig. 1D**) was likely a consequence of the fact that several hydrolysis reactions were required to generate the nucleoside monophosphate product. Consistent with the loss of the intact molecule, the formation of AMP from dsRNA was much slower than ssRNA across the experiment duration, leading to the total combined AMP generated from dsRNA alkaline hydrolysis that was 4.4-fold lower than from ssRNA after 92 h.

2. Hydrolysis of ssRNA and denatured dsRNA at alkaline pH.

At extremely alkaline pH, dsRNA is expected to denature to generate two ssRNA molecules, which we hypothesized will hydrolyze at a similar rate as ssRNA synthesized directly. Using the fact that ssRNA has a 24% higher extinction coefficient compared to dsRNA at 260 nm,[41] we found that both the 100 and 1000 bp dsRNA molecules denatured rapidly when the pH was increased from 12.0 to pH 12.4 (**Fig. S9**), slightly above the pH (~11.8) reported for DNA denaturation.[56,57] We compared the apparent first-order rate constants for hydrolysis of synthetized ssRNA to that of ssRNA generated by dsRNA denaturation for both size ranges at pH 12.4 (**Fig. 2**) using the gel electrophoresis approach. At this higher pH value, ssRNA hydrolysis rate constants increased by ~3-4 fold in comparison to rate constants measured at pH 12.0 **(Fig. 1C & 1E)**, consistent with a 3-fold increase in hydroxide ion concentration. As observed at pH 12.0**,** the hydrolysis rate constants of longer ssRNA were about an order of magnitude higher than those of the shorter ssRNA molecules at pH 12.4 **(Fig. 2)**. We observed that, for both sizes, the hydrolysis rate constant for ssRNA generated by dsRNA denaturation was within 27% of the hydrolysis rate constant for directly synthesized ssRNA. This result indicates that the different hydrolysis rates of ssRNA and dsRNA at pH 12.0 were caused by the double helix structure of dsRNA, rather than their sequence or synthesis procedure, and is consistent our observations that hydrolysis at pH 12.0 is sequence- and synthesis-independent (**Fig. S8**). Given our findings that dsRNA resists hydrolysis at high pH values, the stability of dsRNA at high pH values appears to be limited predominantly by denaturation rather than hydrolysis.

3. Hydrolysis of ssRNA and dsRNA at neutral pH.

We applied our novel findings regarding the ability of dsRNA to resist alkaline hydrolysis to assess the potential rates of dsRNA hydrolysis at circumneutral pH conditions relevant to many

environmental and biological systems. In contrast to pervasive assumptions that dsRNA hydrolysis contributes to rapid dsRNA degradation at these conditions,[34,35] we hypothesized that two factors we observed at high pH would in fact lead to very slow hydrolysis of dsRNA at circumneutral pH. Firstly, as we observed by comparing ssRNA hydrolysis at pH 12.0 to 12.4, the hydrolysis rates of phosphodiester bonds are strongly dependent on pH. Because the concentration of hydroxide ions at pH 7.0 would be 5 orders of magnitude lower than at pH 12.0, the 1006 nt ssRNA molecule, which degraded at pH 12.0 with an apparent rate constant on the order of $\sim 10^{-2}$ min^{-1}, would degrade with an apparent rate constant on the order of $\sim 10^{-7}$ min^{-1} at pH 7.0, corresponding to a half-life of a decade. Secondly, any hydrolysis of the phosphodiester bonds that could occur at circumneutral pH would be further slowed by the duplex structure of dsRNA.

To test our hypothesis that dsRNA hydrolysis will be extremely slow at circumneutral pH, we measured the fraction of dsRNA that remained intact as quantified by our gel electrophoresis approach after incubation at pH 7.0 for 74 days (**Fig. 3**). We determined that neither the 100 bp dsRNA molecule nor the faster-hydrolyzing 1000 bp dsRNA molecule degraded to a measurable extent during the experiment duration. To evaluate whether the stability of dsRNA resulted from slow hydrolysis of RNA at circumneutral pH regardless of structure or the specific stability of dsRNA resulting from its duplex structure, we compared the stability of dsRNA to that of ssRNA at the same experimental conditions. Like the dsRNA molecules, the ssRNA molecules remained intact for the duration of the experiment (**Fig. 3**). These experiments indicate that hydrolysis is slow for both dsRNA and ssRNA at neutral pH. Furthermore, in contrast to prior reports of rapid abiotic degradation of dsRNA products measured by hybridization occurring over days in sterile water,[35] dsRNA molecules in circumneutral solutions free of RNase or other catalyzing agents should be expected to remain intact for long periods of time.

Because neither ssRNA nor dsRNA degraded to a measurable extent at circumneutral pH, we measured the loss of both molecules at moderately alkaline conditions and higher temperatures (pH ~10.0, 50 °C), at which ssRNA would degrade. We determined that 1000 bp dsRNA was not measurably degraded over 5 h, while 1006 nt ssRNA degraded with a rate constant of $3.5(\pm 0.3)\times 10^{-3}$ min^{-1} (**Fig. S11**), consistent with our findings at highly alkaline pH.

4. pH-Dependent abiotic and enzymatic hydrolysis of ssRNA and dsRNA

Because dsRNA resists chemical hydrolysis at neutral and alkaline pH values, its degradation is likely controlled by enzymatic degradation in most environmental and biological systems. In this final experiment, we sought to determine if the unique persistence of dsRNA at alkaline conditions could be exploited to prevent unintended dsRNA degradation by RNase. Here we investigated dsRNA degradation by RNase from two sources: human saliva and agricultural soils. Human saliva is often considered as a source of RNase contamination due to saliva droplets generated by talking and coughing.[58-60] In addition, RNase in agricultural soils may contribute to the unintended degradation of dsRNA pesticides, in particular during extraction prior to analysis.[40]

We first measured the hydrolysis of 1006 nt ssRNA and 1000 bp dsRNA (25 ng/μL) in the presence and absence of human saliva RNase during incubation at 24 °C for 1 h (**Fig. 4A,B**). To enable comparable degradation extents of both ssRNA and dsRNA, we were required to dilute human saliva RNase by 400-fold to degrade ssRNA and only 20-fold to degrade dsRNA. The different dilution factors required suggest that human saliva RNase may be more selective to ssRNA than dsRNA, consistent with RNase from other sources (e.g., human pancreas).[61] Therefore, dsRNA may be more resistant to both enzymatic and alkaline degradation relative to ssRNA. When we compared ssRNA degradation across pH values in the presence of human saliva RNase, we observed that residual ssRNA concentration increased from 8.0(±2.0) ng/μL to 14.4(±2.2) ng/μL ($p = 0.05$) when the pH is increased from 8.0 to 10.0 (**Fig. 4A**). This was likely caused by the decreased saliva RNase activity at higher pH, consistent with RNase sourced from rat serum and insect gut.[62,63] Over the same pH range, ssRNA was not degraded in the absence of RNase. When the pH was increased from pH 10.0 to pH 12.4, the RNase activity decreased further, resulting in higher residual ssRNA concentrations at the higher pH values (**Fig. 4A**). However, the residual ssRNA concentration decreased from below the lowest quantifiable concentration (3.1 ng/μL) when the pH was increased from 10.0 to pH 12.4 in both the presence and absence of RNase, likely due to the significant increase in alkaline hydrolysis rate above pH 10.0. Therefore, in alkaline conditions, abiotic alkaline hydrolysis dominated ssRNA hydrolysis relative to enzymatic hydrolysis.

306 In the absence of human saliva RNase, dsRNA was stable across all pH values below the pH
307 required for dsRNA to denature to ssRNA (i.e., values ⩽ 12.0) (**Fig. 4B**). As expected, increasing the
308 pH further to 12.4 led to rapid hydrolysis of the ssRNA molecules generated from denatured dsRNA,
309 which degraded to below the lowest quantifiable concentration (3.1 ng/μL) like the synthesized ssRNA
310 (**Fig. 4B**). The addition of saliva RNase decreased the residual dsRNA concentration relative to the
311 RNase-free controls to values ranging from 6.9(±1.7) ng/μL to 9.1(±1.2) ng/μL from pH 7.0 to 10.0.
312 Increasing the pH from 10.0 to 12.0 more than doubled the residual concentration of dsRNA from
313 7.7(±0.6) ng/μL to 16.6(±0.3) ng/μL (p = 0.005). The greater residual dsRNA at higher pH values
314 suggests that dsRNA-degrading RNase in saliva may lose activity at elevated pH values. Whereas
315 ssRNA was degraded rapidly at high pH by alkaline hydrolysis despite the loss of RNase activity, the
316 ability of dsRNA to resist alkaline hydrolysis resulted in greater stability at high pH than at
317 circumneutral pH in systems where abiotic and enzymatic reactions co-occur.
318 To test if our findings using human saliva RNase apply to RNase from other sources, we
319 conducted similar experiments using RNase collected from soil at pH 7 (corresponding to the soil pH[40])
320 and pH 11 (corresponding to conditions used to extract dsRNA from soils[40]) at 24 °C **(Fig. 4C and 4D)**.
321 Because RNase activity from the soil was lower than from human saliva, we used a lower initial ssRNA
322 and dsRNA concentration (12.5 ng/μL) and lower dilution factor for the RNase (4-fold to degrade
323 ssRNA and 1.25-fold to degrade dsRNA). Notably, like saliva RNase, soil RNase also appeared to be
324 more selective to ssRNA than dsRNA. We also increased the incubation time from 1 h to 4 h to match
325 the extraction time used for dsRNA quantification in agricultural soils.[40] Under these conditions, the
326 addition of soil RNase at pH 7 decreased the amount of intact ssRNA remaining from 12.9(±0.1) ng/μL
327 to 6.0(±0.6) ng/μL **(Fig. 4C)** and intact dsRNA remaining from 13.2±0.0 ng/μL to 6.5(±0.5) ng/μL
328 **(Fig. 4D)**. At pH 11, ssRNA degraded to a similar extent regardless of the presence or absences of soil
329 RNase, resulting in residual concentrations of 5.8(±0.1) ng/μL and 6.8(±0.2) ng/μL, respectively (**Fig.**
330 **4C)**. Whereas ssRNA degradation at these conditions was dominated by enzymatic hydrolysis at pH 7,
331 alkaline hydrolysis appears to limit ssRNA stability even in the absence of RNase at pH 11. In contrast,
332 dsRNA remained intact regardless of the inclusion or absence of RNase (12.4±0.6 ng/μL and

12.4±1.5 ng/μL, respectively) **(Fig. 4D)**. Consequently, soil RNase, like saliva RNase, appears to be inactivated at high pH, allowing dsRNA to be protected from enzyme degradation without undergoing abiotic alkaline hydrolysis.

5. Environmental implications

In this study, we demonstrated that the unique duplex structure of dsRNA alters its reaction rates and mechanisms relative to ssRNA at alkaline conditions. The slower alkaline hydrolysis rates of dsRNA relative to ssRNA may result from dsRNA adopting a more rigid secondary structure that prevents the intramolecular reaction required for hydrolysis to proceed. As acidic conditions also may catalyze the hydrolysis of phosphodiester bonds (albeit at slower rates than alkaline conditions),[64] dsRNA may also undergo slower acid-catalyzed hydrolysis than ssRNA. However, co-occurring reactions (e.g., depurination) that occur at acidic conditions require additional consideration.[65]

Our finding that dsRNA remained intact in RNase-free and neutral aqueous conditions over months suggests that dsRNA products resist abiotic degradation and should not be assumed to degrade rapidly due to inherent chemical instability. This result challenges previous statements that dsRNA is intrinsically unstable,[34] which should be re-evaluated within the context of the ongoing ecological risk assessment of dsRNA pesticides. Because RNase or other catalyzing agents are required to result in dsRNA degradation in environmental and biological systems, reported dissipation of dsRNA dissipation in autoclaved surface water on the timescale of days[35] might have resulted from RNase contamination, especially considering that some RNases regain activity after autoclaving.[66] Consequently, RNase activity towards dsRNA in receiving environments or tissues[63] likely dominates dsRNA degradation in environmental and biological systems relative to abiotic factors.[67]

Our finding that dsRNA is substantially more stable at high pH than ssRNA enables improved handling, storage, and isolation of dsRNA products used across disciplines. Because ssRNA hydrolyzes faster than dsRNA at elevated pH, incubation at alkaline conditions provides a simple method to remove ssRNA in ssRNA-dsRNA mixture (e.g., during the isolation of viral dsRNA from host cells). In addition, as dsRNA is relatively insensitive to alkaline hydrolysis, unintended dsRNA loss by contaminant RNase may be slowed by working in solutions with alkaline pH, contrary to common suggestions that alkaline

conditions should be avoided for RNA products.[27-31] This strategy may be particularly helpful when there is a risk of RNase contamination, but low-temperature preservation options are not available (e.g., during transportation). Furthermore, when an extraction step is required to transfer adsorbed dsRNA to solution phase prior to quantification,[40] extraction at elevated pH may support increased dsRNA extraction efficiency[40] while suppressing RNase degradation of dsRNA. Extraction at high pH is not applicable to ssRNA in soils due to its vulnerability to alkaline hydrolysis.

Our experimental characterization of ssRNA and dsRNA stability has broad relevance beyond dsRNA products. Some pathogenic waterborne RNA viruses in wastewater could be inactivated by ammonia (NH_3), which in principle may pass through the protein capsid[68,69] and catalyzes RNA hydrolysis via a mechanism analogous to RNA alkaline hydrolysis.[70] Our finding that dsRNA is resistant to chemical hydrolysis relative to ssRNA may explain the finding that dsRNA viruses are less susceptible to this inactivation process than ssRNA viruses.[71] Beyond viral inactivation, our findings on RNA stability may benefit the detection and quantification of virus genetic markers (e.g., ssRNA or dsRNA) that can persist much longer than the infectious viruses in wastewater.[72] Detection of viral genetic markers in wastewater has been applied during outbreaks (e.g., SARS-CoV-2)[73] to enable surveillance, or potential advance notice, of community infection.[74-76] The persistence of viral genetic markers beyond the loss of the infectious viruses may differ between ssRNA and dsRNA due to the different stability of these molecules, such that detection of ssRNA viruses may have a negative bias relative to dsRNA viruses during wastewater surveillance.

Our finding that dsRNA is resistant to alkaline hydrolysis may also allow more accurate evaluations of conditions that could lead to the origin of life. The potential for prebiotic early molecular evolution at alkaline hydrothermal vents (pH 9-11)[77] has been questioned due to the assumed degradation of RNA molecules at alkaline conditions.[78] The insensitivity of dsRNA to alkaline hydrolysis raises the potential that prebiotic RNA in a duplex structure may persist under conditions present in hydrothermal vent conditions.

Supporting Information

Supplementary materials information; sequences of nucleic acids; RNase-free protocol; gel

electrophoresis, RT-qPCR, HPLC analytical method; supplementary results.

Acknowledgments

This work is supported by the Biotechnology Risk Assessment Grant Program Award 2017-33522-26998 from the U.S. Department of Agriculture (K.M.P.), the American Chemical Society Petroleum Research Fund (60057-DNI4) (K.M.P.), and National Science Foundation (MCB-1714352 and MCB-2001743) (T.S.M.). We thank Hani Zaher (Department of Biology, Washington University in St. Louis) for access to qPCR. We thank Fuzhong Zhang (Department of Energy, Environmental & Chemical Engineering, Washington University in St. Louis) for access to the gel image system. We thank Sandra Matteucci (Engineering Communication Center, Washington University in St. Louis) for editing the manuscript.

References

(1) Hannon, G. J., RNA interference. *Nature* **2002,** *418*, 244-251.

(2) Gibori, H.; Eliyahu, S.; Krivitsky, A.; Ben Shushan, D.; Epshtein, Y.; Tiram, G.; Blau, R.; Ofek, P.; Lee, J. S.; Ruppin, E.; Landsman, L.; Barshack, I.; Golan, T.; Merquiol, E.; Blum, G.; Satchi Fainaro, R., Amphiphilic nanocarrier-induced modulation of PLK1 and miR-34a leads to improved therapeutic response in pancreatic cancer. *Nat. Commun.* **2018,** *9*, (1), 16.

(3) Jacque, J. M.; Triques, K.; Stevenson, M., Modulation of HIV-1 replication by RNA interference. *Nature* **2002,** *418*, (6896), 435-438.

(4) Koch, A.; Kogel, K. H., New wind in the sails: improving the agronomic value of crop plants through RNAi-mediated gene silencing. *Plant Biotechnol. J.* **2014,** *12*, (7), 821-831.

(5) Mao, Y. B.; Cai, W. J.; Wang, J. W.; Hong, G. J.; Tao, X. Y.; Wang, L. J.; Huang, Y. P.; Chen, X. Y., Silencing a cotton bollworm P450 monooxygenase gene by plant-mediated RNAi impairs larval tolerance of gossypol. *Nat. Biotechnol.* **2007,** *25*, 1307-1313.

(6) Hunter, W. B.; Glick, E.; Paldi, N.; Bextine, B. R., Advances in RNA interference: dsRNA Treatment in Trees and Grapevines for Insect Pest Suppression. *Southwest. Entomol.* **2012**, (1), 85-87, 3.

(7) Li, H.; Guan, R.; Guo, H.; Miao, X., New insights into an RNAi approach for plant defence against piercing-sucking and stem-borer insect pests. *Plant Cell Environ.* **2015,** *38*, (11), 2277-2285.

(8) Cagliari, D.; Dias, N. P.; Galdeano, D. M.; dos Santos, E. Á.; Smagghe, G.; Zotti, M. J., Management of Pest Insects and Plant Diseases by Non-Transformative RNAi. *Front. Plant Sci.* **2019,** *10*, 1319.

(9) Mitter, N.; Worrall, E. A.; Robinson, K. E.; Li, P.; Jain, R. G.; Taochy, C.; Fletcher, S. J.; Carroll, B. J.; Lu, G. Q.; Xu, Z. P., Clay nanosheets for topical delivery of RNAi for sustained protection against plant viruses. *Nat. Plants* **2017,** *3*, 16207.

(10) Li, Y.; Breaker, R. R., Kinetics of RNA Degradation by Specific Base Catalysis of Transesterification Involving the 2‘-Hydroxyl Group. *J. Am. Chem. Soc.* **1999,** *121*, (23), 5364-5372.

(11) Usher, D. A., RNA Double Helix and the Evolution of the 3′,5′ Linkage. *Nat. New Biol.* **1972,**

426 *235*, (59), 207-208.
427 (12) Kierzek, R., Nonenzymatic hydrolysis of oligoribonucleotides. *Nucleic Acids Res.* **1992,** *20*,
428 (19), 5079-5084.
429 (13) Kaukinen, U.; Lyytikäinen, S.; Mikkola, S.; Lönnberg, H., The reactivity of phosphodiester
430 bonds within linear single-stranded oligoribonucleotides is strongly dependent on the base sequence.
431 *Nucleic Acids Res.* **2002,** *30*, (2), 468-474.
432 (14) Soukup, G. A.; Breaker, R. R., Relationship between internucleotide linkage geometry and the
433 stability of RNA. *RNA* **1999,** *5*, (10), 1308-1325.
434 (15) Ciesiolka, J.; Lorenz, S.; Erdmann, V. A., Different conformational forms of *Escherichia coli*
435 and rat liver 5S rRNA revealed by Pb(II)-induced hydrolysis. *Eur. J. Biochem.* **1992,** *204*, (2), 583-589.
436 (16) Ciesiołka, J.; Michałowski, D.; Wrzesinski, J.; Krajewski, J.; Krzyżosiak, W. J., Patterns of
437 cleavages induced by lead ions in defined RNA secondary structure motifs. *J. Mol. Biol.* **1998,** *275*, (2),
438 211-220.
439 (17) Das, P. R.; Sherif, S. M., Application of Exogenous dsRNAs-induced RNAi in Agriculture:
440 Challenges and Triumphs. *Front. Plant Sci.* **2020,** *11*, 946.
441 (18) Dow, J. A. T., Insect Midgut Function. In *Adv. Insect Physiol.*; Evans, P. D.; Wigglesworth, V.
442 B., Eds.; Academic Press: 1987; Vol. 19, pp 187-328.
443 (19) Dow, J. A., Extremely high pH in biological systems: a model for carbonate transport. *Am. J.*
444 *Physiol. Regul. Integr. Comp. Physiol.* **1984,** *246*, (4), R633-R636.
445 (20) Christiaens, O.; Swevers, L.; Smagghe, G., DsRNA degradation in the pea aphid
446 (*Acyrthosiphon pisum*) associated with lack of response in RNAi feeding and injection assay. *Peptides*
447 **2014,** *53*, 307-314.
448 (21) Christiaens, O.; Tardajos, M. G.; Martinez Reyna, Z. L.; Dash, M.; Dubruel, P.; Smagghe, G.,
449 Increased RNAi Efficacy in *Spodoptera exigua* via the Formulation of dsRNA With Guanylated
450 Polymers. *Front. Physiol.* **2018,** *9*, 316.
451 (22) Price, D. R. G.; Gatehouse, J. A., RNAi-mediated crop protection against insects. *Trends*
452 *Biotechnol.* **2008,** *26*, (7), 393-400.

(23) Lim, Z. X.; Robinson, K. E.; Jain, R. G.; Sharath Chandra, G.; Asokan, R.; Asgari, S.; Mitter, N., Diet-delivered RNAi in *Helicoverpa armigera* – Progresses and challenges. *J. Insect Physiol.* **2016,** *85*, 86-93.

(24) Swevers, L.; Smagghe, G., Use of RNAi for Control of Insect Crop Pests. In *Arthropod-Plant Interactions: Novel Insights and Approaches for IPM*; Smagghe, G.; Diaz, I., Eds.; Springer Netherlands: Dordrecht, 2012; pp 177-197.

(25) Liu, S.; Jaouannet, M.; Dempsey, D. M. A.; Imani, J.; Coustau, C.; Kogel, K.-H., RNA-based technologies for insect control in plant production. *Biotechnol. Adv.* **2020,** *39*, 107463.

(26) Cooper, A. M.; Silver, K.; Zhang, J.; Park, Y.; Zhu, K. Y., Molecular mechanisms influencing efficiency of RNA interference in insects. *Pest Manage. Sci.* **2019,** *75*, (1), 18-28.

(27) Brown, T.; Mackey, K.; Du, T., Analysis of RNA by Northern and Slot Blot Hybridization. *Curr. Protoc. Mol. Biol.* **2004,** *67*, (1), 4.9.1-4.9.19.

(28) Wozniak, A.; Cerda, A.; Ibarra Henriquez, C.; Sebastian, V.; Armijo, G.; Lamig, L.; Miranda, C.; Lagos, M.; Solari, S.; Guzmán, A. M.; Quiroga, T.; Hitschfeld, S.; Riveras, E.; Ferres, M.; Gutiérrez, R. A.; García, P., A simple RNA preparation method for SARS-CoV-2 detection by RT-qPCR. *Sci. Rep.* **2020,** *10*, (1), 16608. 10.1038/s41598-020-73616-w

(29) New England Biolabs, A Practical Guide to Analyzing Nucleic Acid Concentration and Purity with Microvolume Spectrophotometers. Available at https://www.neb.com/-/media/catalog/application-notes/mvs_analysis_of_na_concentration_and_purity.pdf?rev=be7c8e19f4d34e558527496ea51623dc. Accessed 10 September 2020.

(30) ThermoFisher, The Basics: RNA Isolation. https://www.thermofisher.com/us/en/home/references/ambion-tech-support/rna-isolation/general-articles/the-basics-rna-isolation.html. Accessed 20 September 2020.

(31) LifeScience, Precautions for Handling of RNA. Available at https://lifescience.roche.com/en_us/articles/precautions-for-handling-of-rna.html. Accessed 20 September 2020.

(32) New England Biolabs, Product Information of dsRNA laddder (N0363S). Available at https://www.neb.com/products/n0363-dsrna-ladder#Product%20Information. Accessed 12 October 2020.

(33) ThermoFisher, MEGAscript™ RNAi Kit Instruction Manual. Available at https://assets.thermofisher.com/TFS-Assets/LSG/manuals/cms_072987.pdf. Accessed 26 August 2020.

(34) United States Environmental Protection Agency, SAP Minutes No. 2014-02, A Set of Scientific Issues Being Considered by The Environmental Protection Agency Regarding: RNAi Technology as a Pesticide: Problem Formulation for Human Health and Ecological Risk Assessment (Arlington, VA, 2014).

(35) Albright, V. C.; Wong, C. R.; Hellmich, R. L.; Coats, J. R., Dissipation of double-stranded RNA in aquatic microcosms. *Environ. Toxicol. Chem.* **2017,** *36*, (5), 1249-1253.

(36) Parker, K. M.; Barragán Borrero, V.; van Leeuwen, D. M.; Lever, M. A.; Mateescu, B.; Sander, M., Environmental fate of RNA interference pesticides: Adsorption and degradation of double-stranded RNA molecules in agricultural soils. *Environ. Sci. Technol.* **2019,** *53*, (6), 3027-3036.

(37) Masek, T.; Vopalensky, V.; Suchomelova, P.; Pospisek, M., Denaturing RNA electrophoresis in TAE agarose gels. *Anal. Biochem.* **2005,** *336*, (1), 46-50.

(38) Bradbury, S., Human Saliva as a Convenient Source of Ribonuclease. *J. Cell Sci.* **1956,** *s3-97*, (39), 323-327.

(39) Bardoń, A.; Shugar, D., Properties of purified salivary ribonuclease, and salivary ribonuclease levels in children with cystic fibrosis and in heterozygous carriers. *Clin. Chim. Acta* **1980,** *101*, (1), 17-24.

(40) Zhang, K.; Wei, J.; Huff Hartz, K. E.; Lydy, M. J.; Moon, T. S.; Sander, M.; Parker, K. M., Analysis of RNA Interference (RNAi) Biopesticides: Double-Stranded RNA (dsRNA) Extraction from Agricultural Soils and Quantification by RT-qPCR. *Environ. Sci. Technol.* **2020,** *54*, (8), 4893-4902.

(41) Nwokeoji, A. O.; Kilby, P. M.; Portwood, D. E.; Dickman, M. J., Accurate Quantification of Nucleic Acids Using Hypochromicity Measurements in Conjunction with UV Spectrophotometry. *Anal. Chem.* **2017,** *89*, (24), 13567-13574.

(42) Velikyan, I.; Acharya, S.; Trifonova, A.; Földesi, A.; Chattopadhyaya, J., The pKa's of 2'-Hydroxyl Group in Nucleosides and Nucleotides. *J. Am. Chem. Soc.* **2001,** *123*, (12), 2893-2894.

(43) Oivanen, M.; Kuusela, S.; Lönnberg, H., Kinetics and Mechanisms for the Cleavage and Isomerization of the Phosphodiester Bonds of RNA by Brønsted Acids and Bases. *Chem. Rev.* **1998,** *98*, (3), 961-990.

(44) Bock, R. M., Alkaline hydrolysis of RNA. In *Methods Enzymol.*; Grossman, L.; Moldave, K., Eds.; Academic Press: New York, U.S.A., 1967; Vol. 12, pp 224-228.

(45) Kauffmann, A. D.; Campagna, R. J.; Bartels, C. B.; Childs-Disney, J. L., Improvement of RNA secondary structure prediction using RNase H cleavage and randomized oligonucleotides. *Nucleic Acids Res.* **2009,** *37*, (18), e121-e121.

(46) Puglisi, J. D.; Tinoco, I., Absorbance melting curves of RNA. In *Methods Enzymol.*; Academic Press: 1989; Vol. 180, pp 304-325.

(47) Lorenz, R.; Bernhart, S. H.; Höner zu Siederdissen, C.; Tafer, H.; Flamm, C.; Stadler, P. F.; Hofacker, I. L., ViennaRNA Package 2.0. *Algorithms Mol. Biol.* **2011,** *6*, (1), 26.

(48) Zhang, K.; Li, H.; Chen, W.; Zhao, M.; Cui, H.; Min, Q.; Wang, H.; Chen, S.; Li, D., Regulation of the Docosapentaenoic Acid/Docosahexaenoic Acid Ratio (DPA/DHA Ratio) in *Schizochytrium limacinum* B4D1. *Appl. Biochem. Biotechnol.* **2017,** *182*, (1), 67-81.

(49) Du, H.; Liao, X.; Gao, Z.; Li, Y.; Lei, Y.; Chen, W.; Chen, L.; Fan, X.; Zhang, K.; Chen, S.; Ma, Y.; Meng, C.; Li, D., Effects of Methanol on Carotenoids as Well as Biomass and Fatty Acid Biosynthesis in *Schizochytrium limacinum* B4D1. *Appl. Environ. Microbiol.* **2019,** *85*, (19), e01243-19.

(50) Thornton, B.; Basu, C., Rapid and Simple Method of qPCR Primer Design. In *PCR Primer Design*; Basu, C., Ed; Springer New York: New York, NY, 2015; pp 173-179.

(51) Livak, K. J.; Schmittgen, T. D., Analysis of Relative Gene Expression Data Using Real-Time Quantitative PCR and the $2^{-\Delta\Delta CT}$ Method. *Methods* **2001,** *25*, (4), 402-408.

(52) Brown, D. M.; Todd, A. R., 13. Nucleotides. Part X. Some observations on the structure and chemical behaviour of the nucleic acids. *J. Chem. Soc. (Resumed)* **1952**, (0), 52-58.

(53) Komiyama, M.; Takeshige, Y., Regioselective phosphorus-oxygen(3') cleavage of 2',3'-cyclic

534 monophosphates of ribonucleosides catalyzed by β- and γ-cyclodextrins. *J. Org. Chem.* **1989,** *54*, (20),
535 4936-4939.
536 (54) Dugas, H.; Penney, C., Bioorganic Chemistry of the Phosphates. In *Bioorganic Chemistry: A*
537 *Chemical Approach to Enzyme Action*; Springer US: New York, NY, 1981; pp 93-178.
538 (55) Komiyama, M.; Yoshinari, K., Kinetic Analysis of Diamine-Catalyzed RNA Hydrolysis. *J. Org.*
539 *Chem.* **1997,** *62*, (7), 2155-2160.
540 (56) Ageno, M.; Dore, E.; Frontali, C., The Alkaline Denaturation of DNA. *Biophys. J.* **1969,** *9*, (11),
541 1281-1311.
542 (57) Ehrlich, P.; Doty, P., The Alkaline Denaturation of Deoxyribose Nucleic Acid. *J. Am. Chem.*
543 *Soc.* **1958,** *80*, (16), 4251-4255.
544 (58) Wang, S., Single Molecule RNA FISH (smFISH) in Whole-Mount Mouse Embryonic Organs.
545 *Curr. Protoc. Cell Biol.* **2019,** *83*, (1), e79.
546 (59) Qiagen, The DO's and DON'Ts of working with RNA. Available at
547 www.qiagen.com/us/resources/download.aspx?id=d86e4457-e017-4f4a-84f9-8f5e2e2297e0&lang=en.
548 Accessed 12 October 2020.
549 (60) Lee, D.; Xiong, S.; Xiong, W. C., General Introduction to In Situ Hybridization Protocol Using
550 Nonradioactively Labeled Probes to Detect mRNAs on Tissue Sections. In *Neural Development:*
551 *Methods and Protocols*; Zhou, R.; Mei, L., Eds.; Humana Press: Totowa, NJ, 2013; pp 165-174.
552 (61) Sorrentino, S.; Libonati, M., Human Pancreatic-Type and Nonpancreatic-Type Ribonucleases:
553 A Direct Side-by-Side Comparison of Their Catalytic Properties. *Arch. Biochem. Biophys.* **1994,** *312*,
554 (2), 340-348.
555 (62) Umeda, T.; Moriyama, T.; Oura, H.; Tsukada, K., Rat serum ribonuclease. *BBA-Enzymology*
556 **1969,** *171*, (2), 260-264.
557 (63) Peng, Y.; Wang, K.; Fu, W.; Sheng, C.; Han, Z., Biochemical Comparison of dsRNA
558 Degrading Nucleases in Four Different Insects. *Front. Physiol.* **2018,** *9*, 624.
559 (64) Jarvinen, P.; Oivanen, M.; Lonnberg, H., Interconversion and phosphoester hydrolysis of 2',5'-
560 and 3',5'-dinucleoside monophosphates: kinetics and mechanisms. *J. Org. Chem.* **1991,** *56*, (18), 5396-

561 5401.
562 (65) An, R.; Jia, Y.; Wan, B.; Zhang, Y.; Dong, P.; Li, J.; Liang, X., Non-Enzymatic Depurination
563 of Nucleic Acids: Factors and Mechanisms. *PLoS One* **2015,** *9*, (12), e115950.
564 (66) Miyamoto, T.; Okano, S.; Kasai, N., Irreversible thermoinactivation of ribonuclease-A by soft-
565 hydrothermal processing. *Biotechnol. Prog.* **2009,** *25*, (6), 1678-1685.
566 (67) Parker, K. M.; Sander, M., Environmental Fate of Insecticidal Plant-Incorporated Protectants
567 from Genetically Modified Crops: Knowledge Gaps and Research Opportunities. *Environ. Sci. Technol.*
568 **2017,** *51*, (21), 12049-12057.
569 (68) Goncharova, E. P.; Kovpak, M. P.; Ryabchikova, E. I.; Konevets, D. A.; Sil'nikov, V. N.;
570 Zenkova, M. A.; Vlasov, V. V., Viral genome cleavage with artificial ribonucleases: A new method to
571 inactivate RNA-containing viruses. *Dokl. Biochem. Biophys.* **2009,** *427*, (1), 221-224.
572 (69) Broo, K.; Wei, J.; Marshall, D.; Brown, F.; Smith, T. J.; Johnson, J. E.; Schneemann, A.;
573 Siuzdak, G., Viral capsid mobility: A dynamic conduit for inactivation. *Proc. Natl. Acad. Sci. U.S.A.*
574 **2001,** *98*, (5), 2274-2277.
575 (70) Decrey, L.; Kazama, S.; Udert, K. M.; Kohn, T., Ammonia as an In Situ Sanitizer: Inactivation
576 Kinetics and Mechanisms of the ssRNA Virus MS2 by NH_3. *Environ. Sci. Technol.* **2015,** *49*, (2), 1060-
577 1067.
578 (71) Magri, M. E.; Fidjeland, J.; Jönsson, H.; Albihn, A.; Vinnerås, B., Inactivation of adenovirus,
579 reovirus and bacteriophages in fecal sludge by pH and ammonia. *Sci. Total Environ.* **2015,** *520*, 213-
580 221.
581 (72) Bivins, A.; Greaves, J.; Fischer, R.; Yinda, K. C.; Ahmed, W.; Kitajima, M.; Munster, V. J.;
582 Bibby, K., Persistence of SARS-CoV-2 in Water and Wastewater. *Environ. Sci. Technol. Lett* **2020,** *7*,
583 (12), 937–942.
584 (73) Foladori, P.; Cutrupi, F.; Segata, N.; Manara, S.; Pinto, F.; Malpei, F.; Bruni, L.; La Rosa, G.,
585 SARS-CoV-2 from faeces to wastewater treatment: What do we know? A review. *Sci. Total Environ.*
586 **2020,** *743*, 140444.
587 (74) Lodder, W.; de Roda Husman, A. M., SARS-CoV-2 in wastewater: potential health risk, but

588 also data source. *Lancet Gastroenterol. Hepatol.* **2020,** *5*, (6), 533-534.
589 (75) Peccia, J.; Zulli, A.; Brackney, D. E.; Grubaugh, N. D.; Kaplan, E. H.; Casanovas Massana, A.;
590 Ko, A. I.; Malik, A. A.; Wang, D.; Wang, M.; Warren, J. L.; Weinberger, D. M.; Arnold, W.; Omer, S.
591 B., Measurement of SARS-CoV-2 RNA in wastewater tracks community infection dynamics. *Nat.*
592 *Biotechnol.* **2020,** *38*, (10), 1164-1167.
593 (76) Randazzo, W.; Truchado, P.; Cuevas-Ferrando, E.; Simón, P.; Allende, A.; Sánchez, G., SARS-
594 CoV-2 RNA in wastewater anticipated COVID-19 occurrence in a low prevalence area. *Water Res.*
595 **2020,** *181*, 115942.
596 (77) Martin, W.; Baross, J.; Kelley, D.; Russell, M. J., Hydrothermal vents and the origin of life.
597 *Nat. Rev. Microbiol* **2008,** *6*, (11), 805-814.
598 (78) Le Vay, K.; Salibi, E.; Song, E. Y.; Mutschler, H., Nucleic Acid Catalysis under Potential
599 Prebiotic Conditions. *Chem. Asian J.* **2020,** *15*, (2), 214-230.
600

601 **TOC**

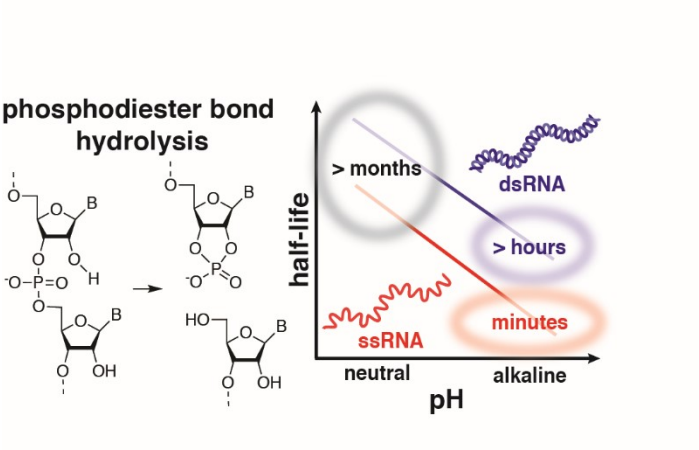
phosphodiester bond
hydrolysis
half-life
> months
dsRNA
> hours
minutes
ssRNA
neutral
alkaline
pH

602

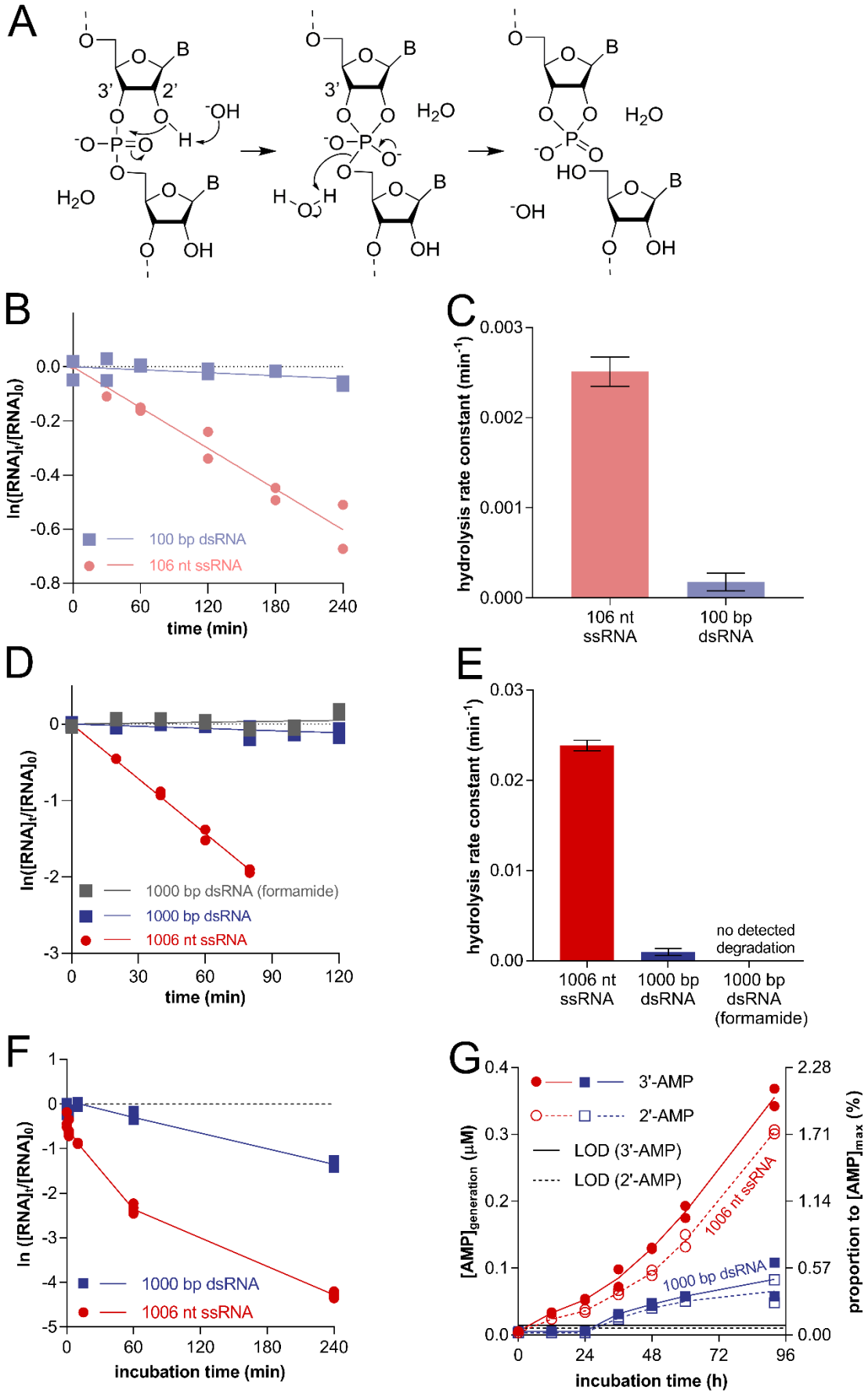
A
B
100 bp dsRNA
106 nt ssRNA
ln([RNA]t/[RNA]0)
time (min)
C
hydrolysis rate constant (min-1)
106 nt ssRNA
100 bp dsRNA
D
1000 bp dsRNA (formamide)
1000 bp dsRNA
1006 nt ssRNA
time (min)
E
hydrolysis rate constant (min-1)
no detected degradation
1006 nt ssRNA
1000 bp dsRNA
1000 bp dsRNA (formamide)
F
ln ([RNA]t/[RNA]0)
1000 bp dsRNA
1006 nt ssRNA
incubation time (min)
G
3'-AMP
2'-AMP
LOD (3'-AMP)
LOD (2'-AMP)
1006 nt ssRNA
1000 bp dsRNA
[AMP]generation (µM)
proportion to [AMP]max (%)
incubation time (h)

Fig. 1. Hydrolysis of ssRNA and dsRNA at alkaline pH. (**A**) Alkaline hydrolysis of phosphodiester bonds.[10] B represents nucleotide base moieties (A, U, G, or C). The generated 2',3'-cyclic phosphate terminus will then hydrolyze to 2' and 3'-phosphate termini. (**B-E**) RNA loss (initial concentration = 25 ng/μL) in solutions containing 20 mM NaCl, and 3 mM phosphate at pH 12.0 and 24 °C measured by agarose gel electrophoresis. Reactions were ended by adjusting the sample to neutral pH. Two independent samples were prepared for each time point. (**B, D**) Lines were generated by fitting all the data in the same group. The slopes of the best-fitted lines and their standard errors are indicated as hydrolysis rate constants and error bars in (**C**) and (**E**), respectively. In the 1000 bp dsRNA formamide group, the incubation was the same as the 1000 bp dsRNA group, but a formamide treatment was added. The hydrolyzed 1006 nt ssRNA concentration at 100 and 120 min was lower than the lowest quantifiable concentration (3.1 ng/μL). (**F**) RNA loss (initial concentration = 1 ng/μL) in identical solutions as above analyzed by RT-qPCR. Lines in the figures connect the averages of four independent samples. (**G**) Product formation from RNA (initial concentration = 25 ng/μL) in identical solutions as above analyzed by HPLC. Lines in the figures connect the averages of two independent samples. $[AMP]_{max}$ denotes the AMP concentration when RNA molecules were fully hydrolyzed to nucleoside monophosphate. To calculate the proportion to $[AMP]_{max}$, we used the average value (17.48 μM) for ssRNA and dsRNA, which have $[AMP]_{max}$ values of 17.04 and 17.92 μM, respectively.

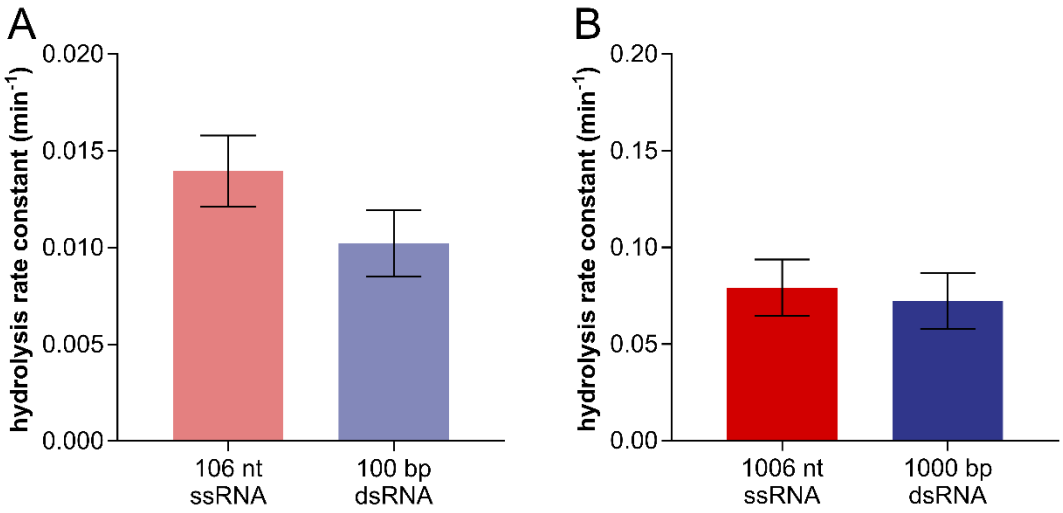

621

622 **Fig. 2.** Hydrolysis rate constant of ssRNA and denatured dsRNA at pH 12.4 and 24 °C. The RNA
623 hydrolysis reaction contained 25 ng/μL RNA, 20 mM NaCl, and 3 mM phosphate. Reactions were
624 ended by adjusting the sample to neutral pH. RNA concentration after hydrolysis was measured by
625 agarose gel electrophoresis. Rate constants and their standard errors (indicated as error bars) were
626 determined from two individual samples for timepoints ranging from 1-30 min (A) and 0.5-6 min (B)
627 (visualized in **Fig. S12**).

628

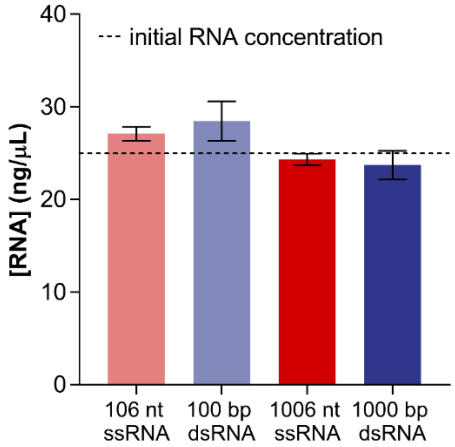

629

630 **Fig. 3.** Analysis of ssRNA and dsRNA by agarose gel electrophoresis after 74 days of incubation at pH
631 7.0 and 24 °C. The reaction contained 25 ng/μL RNA, 20 mM NaCl, and 3 mM MOPS. Error bars
632 represent the standard deviations of measurements from eight independently prepared samples. The
633 initial RNA concentration refers to the nominal value.

634

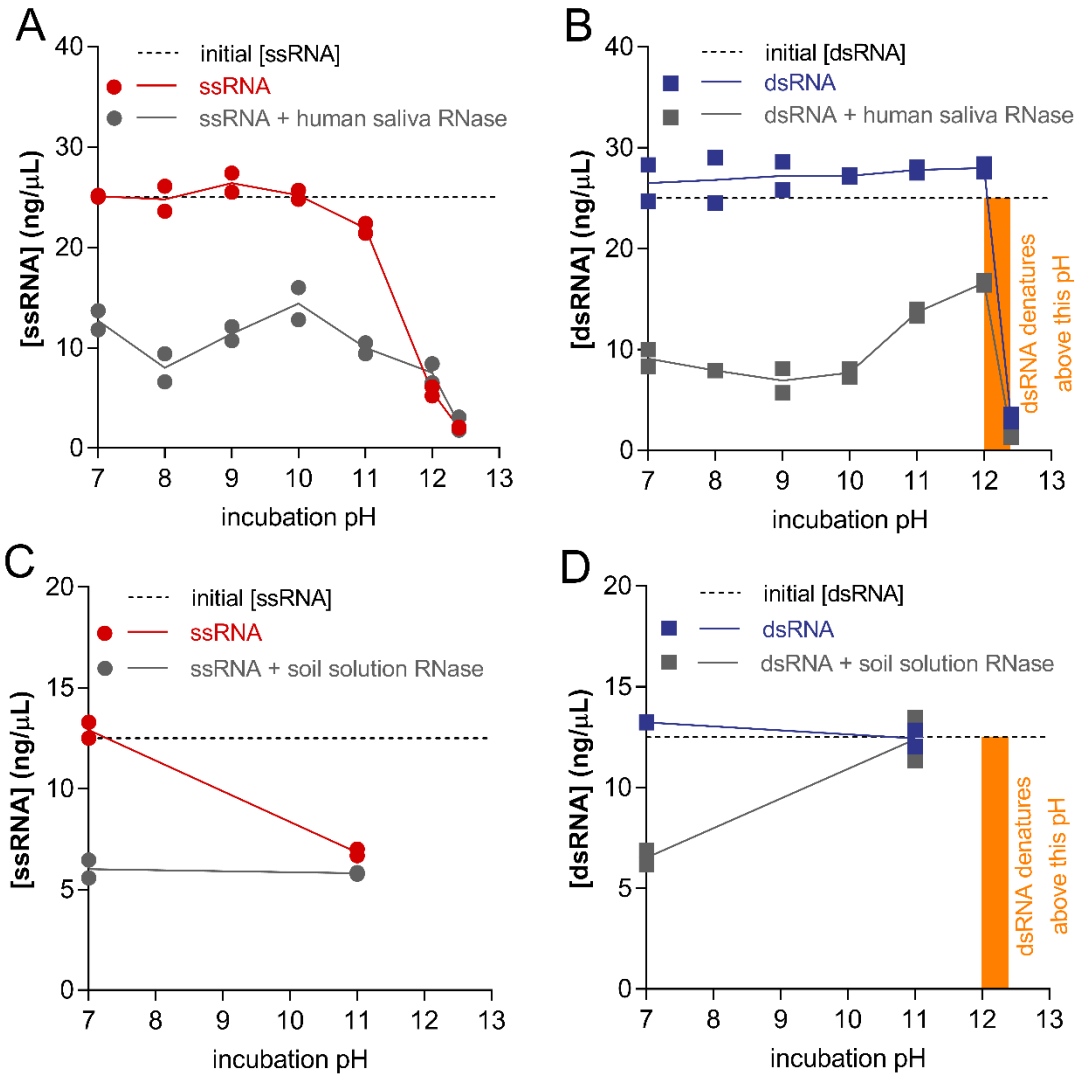

635

636 **Fig. 4.** Analysis of 1006 nt ssRNA (**A**, **C**) and 1000 bp dsRNA (**B**, **D**) by agarose gel electrophoresis
637 after incubation at 24 °C for 1 h (**A**, **B**) or 4 h (**C**, **D**). The RNA hydrolysis reaction (20 µL) contained
638 25.0 ng/µL (A, B) or 12.5 ng/µL (C, D) RNA, 20 mM NaCl, and 3 mM buffer salt (MOPS for pH 7.0-
639 8.0, borate for pH 9.0, bicarbonate for pH 10.0-11.0 and phosphate for pH 12.0-12.4). Human saliva
640 RNase was 400-fold (**A**) or 20-fold (**B**) diluted. Soil solution RNase was 4-fold (**C**) or 1.25-fold (**D**).
641 Two independent samples were prepared for each condition. Lines in the figures connect the averages.
642 Reactions were ended by storing (for ~10 min) the samples in a pre-cooled (-20 °C) cooler before
643 loading them into gels. The lowest quantifiable concentration was 3.1 ng/µL RNA in gels. The initial
644 RNA concentration refers to the nominal value.